

Supplemental Figures

Figure S1

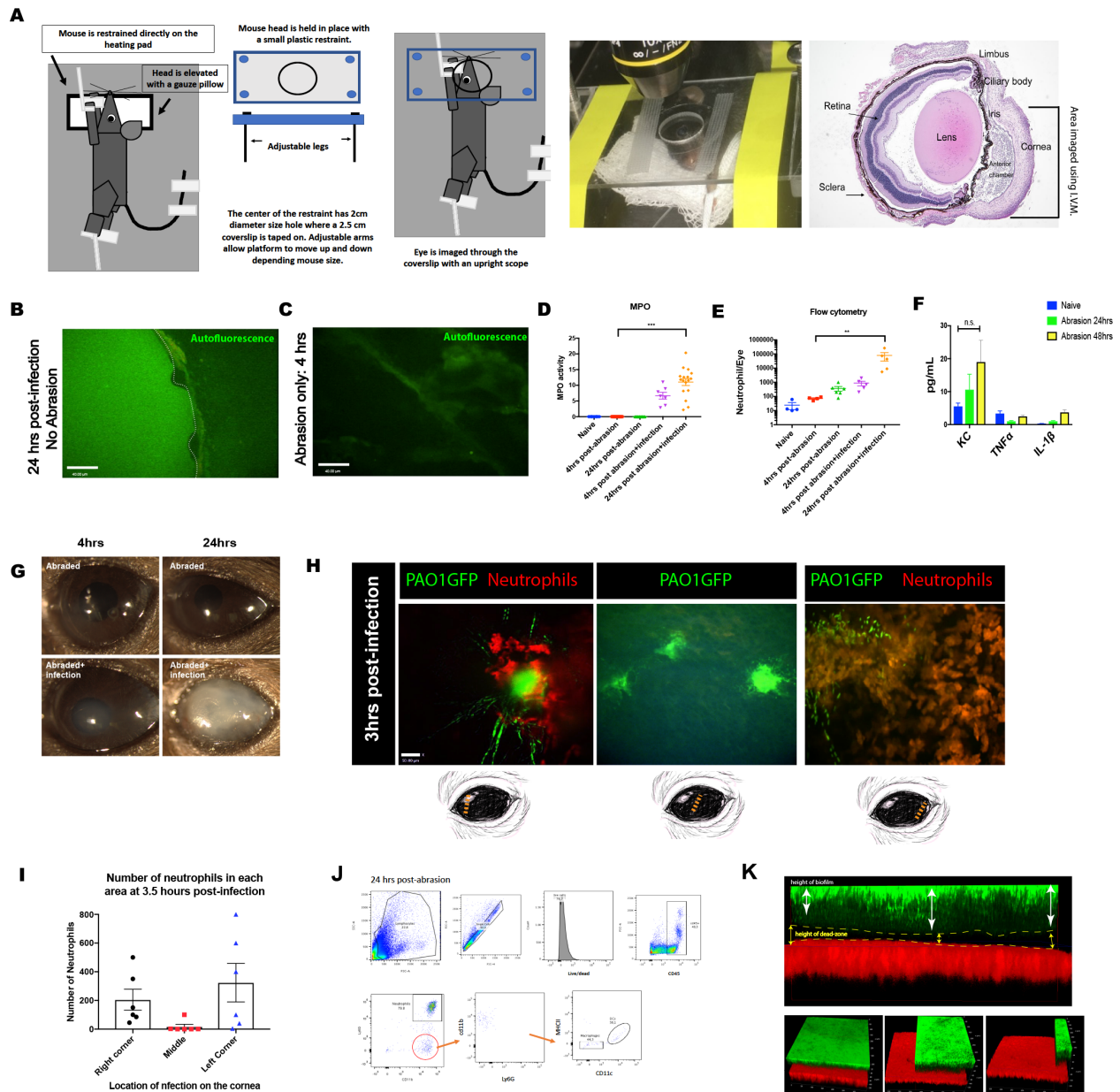


Figure S1. Development of intravital imaging of the cornea to visualize the movement of ocular neutrophils. Related to Figure 1 and STAR methods: Eye Intravital microscopy. **A.** Intravital microscopy (IVM) set up for upright imaging systems (Leica SP8 and spinning-disk (SD) confocal). **B.** IVM-SD image of corneas 24 hours post-infection, no eye abrasions were performed on these mice. **C.** IVM-SD of corneas that were abraded (using full abrasion model) after 4 hours. **D.** Myeloperoxidase activity in the eye after abrasion alone or abrasion

+infection. **E.** Neutrophil numbers in the eye after abrasion or abrasion + infection using flow cytometry. **F.** Concentration of pro-inflammatory cytokines/chemokines in the eye after abrasion. **G.** Image of eyes at 4, 24 hours post-abrasion as well as post-abrasion + infection. **H.** Multiple isolated small abrasions were made on the surface of the mouse eye and infected. Neutrophil recruitment was tracked using IVM-SD at 3 hours for 30 minutes. N=3. **I.** Quantification of neutrophil numbers by IVM at different sites on the cornea at 3.5 hours post-infection. **J.** Flow cytometry gating strategy used. **K.** Strategy used to quantify biofilm and dead-zone size. Data in D, E, F, and I are represented as the mean \pm standard error and tested by one-way ANOVA. * $p < 0.05$; ** $p < 0.01$, *** $p < 0.001$. n=6-8 per group.

Figure S2

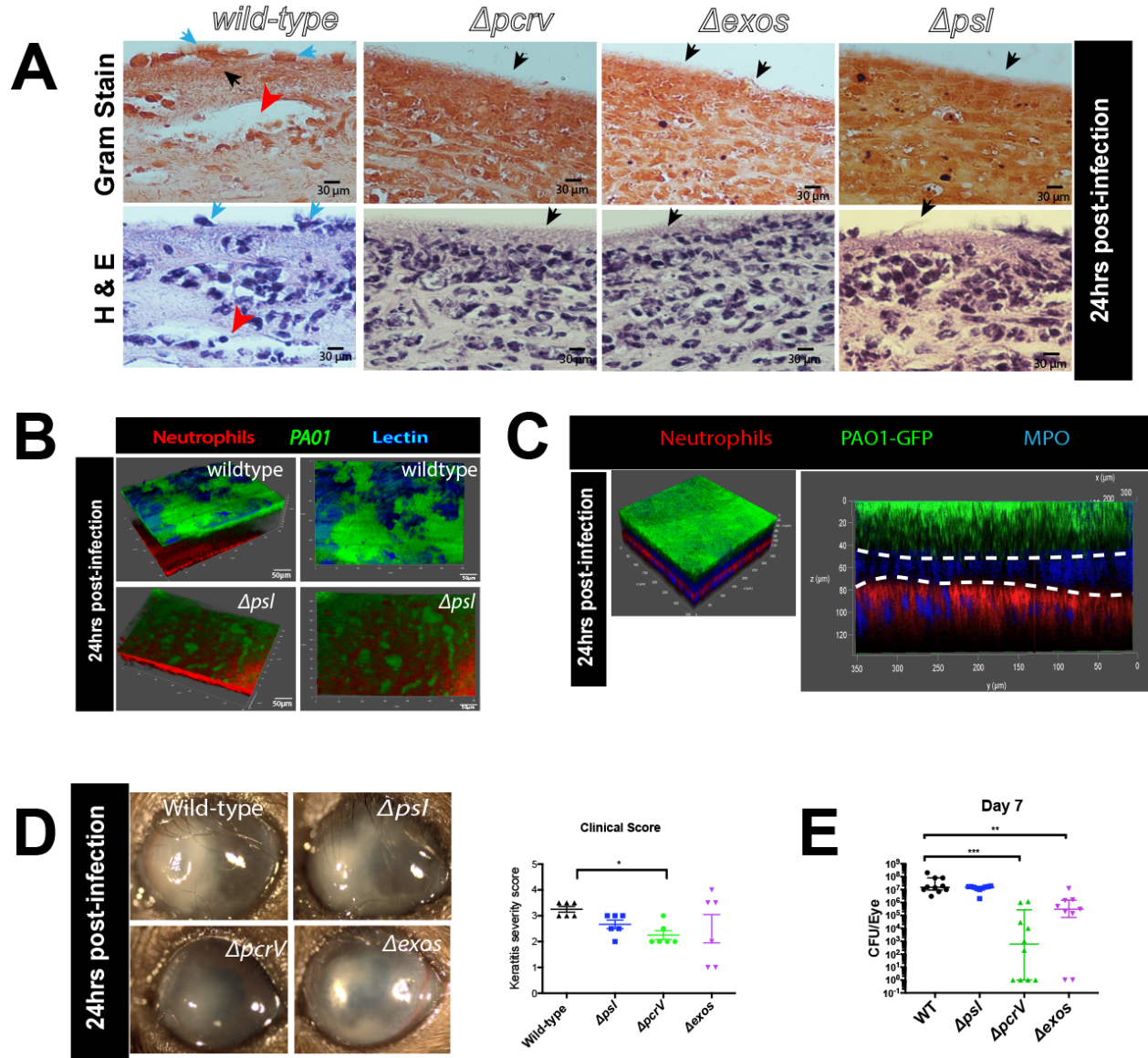


Figure S2. In the absence of T3S effector ExoS, the dead-zone is no longer formed. Related to Figure 2. A. Paraffin sections of eyes extracted from mice infected for 24 hours with wild-type or mutant *P. aeruginosa* strains. Top panel shows samples stained with Gram-stain while the bottom panel shows samples stained with hematoxylin and eosin. Black arrows are directed toward bacteria, red arrow is directed towards the dead-zone, blue arrows define cross-sections of the mushroom structures seen by electron microscopy on the surface of the cornea (as seen in Figure 1G). **B.** 3D reconstruction visualizing lectin stain on biofilms formed by wild-

type mice. *P. aeruginosa* (green), neutrophils (red), MOA lectin (blue). **C.** Myeloperoxidase staining in the dead-zone. *P. aeruginosa* (green), neutrophils (red), MPO (blue). **D.** Clinical keratitis scores for eyes were assessed at 24hours post-infection with wildtype and mutant bacterial strains. **E.** Quantification of bacterial CFUs in eyes at 7 days post-infection. All experiments were performed with the full abrasion model described in the methods section. Data in E are represented as median and interquartile range and tested by non-parametric Kruskal-Wallis ANOVA, n=4-5 mice per group. Data in D are represented as the mean \pm standard error and tested by one-way ANOVA. *p<0.05; **p<0.01, ***p<0.001.

Figure S3

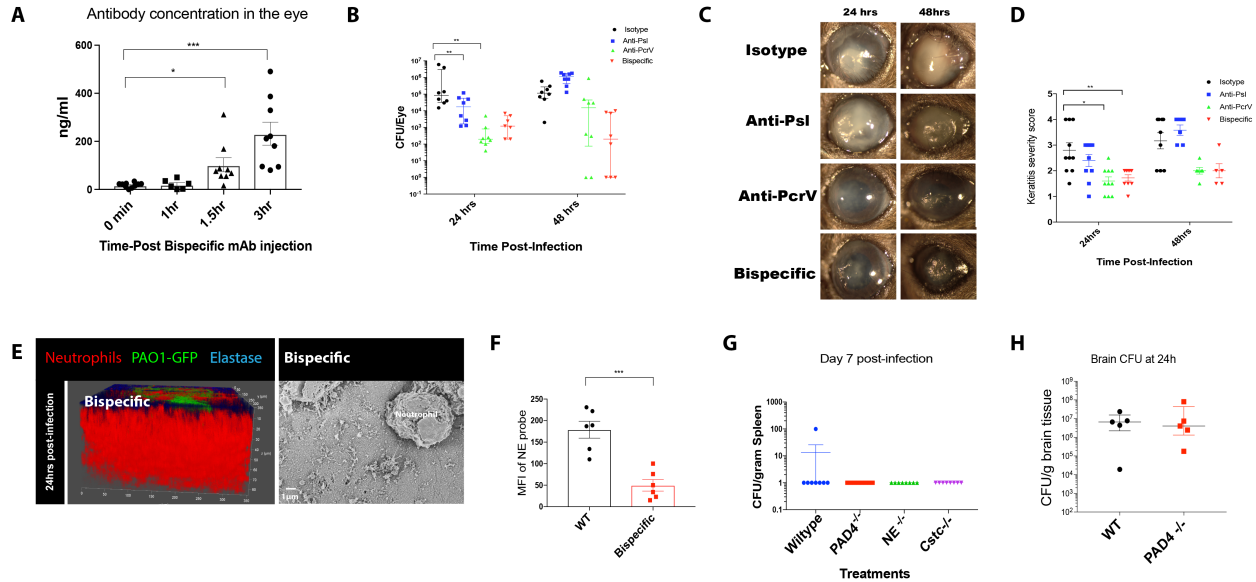


Figure S3. The therapeutic bispecific antibody (MEDI3902), rapidly enters the eye and reduces keratitis severity starting at 24 hours post-infection. Related to Figure 4. A. Quantification of bispecific antibody in the eye after systemic administration. **B.** Quantification of bacterial CFUs in eyes at 24- and 48-hours post-infection. **C.** Representative images of eyes to determine eye pathology scores **D.** Clinical scores for keratitis severity (24 hours n=10, 48 hours n=6). **E.** 3D multiphoton image (left) and scanning electron image (right) of the eye 24 hours post-abrasion + infection in a mouse prophylactically treated with bispecific antibody. **F.** Quantification of neutrophil elastase probe staining. **G.** Quantification of bacterial CFUs in spleens at 7 days post ocular infection. **H.** Quantification of bacterial CFUs in brains 24 hours after 500 CFU of *P. aeruginosa* was injected directly into the brain. All experiments were performed with full abrasion model described in the methods section. Data in B, G, and H are represented as median and interquartile range and tested by non-parametric Kruskal-Wallis ANOVA. Data in A, D and F are represented as the mean \pm standard error and tested by one-way ANOVA. * $p < 0.05$; ** $p < 0.01$, *** $p < 0.001$. n=5 per group unless otherwise stated.

Figure S4

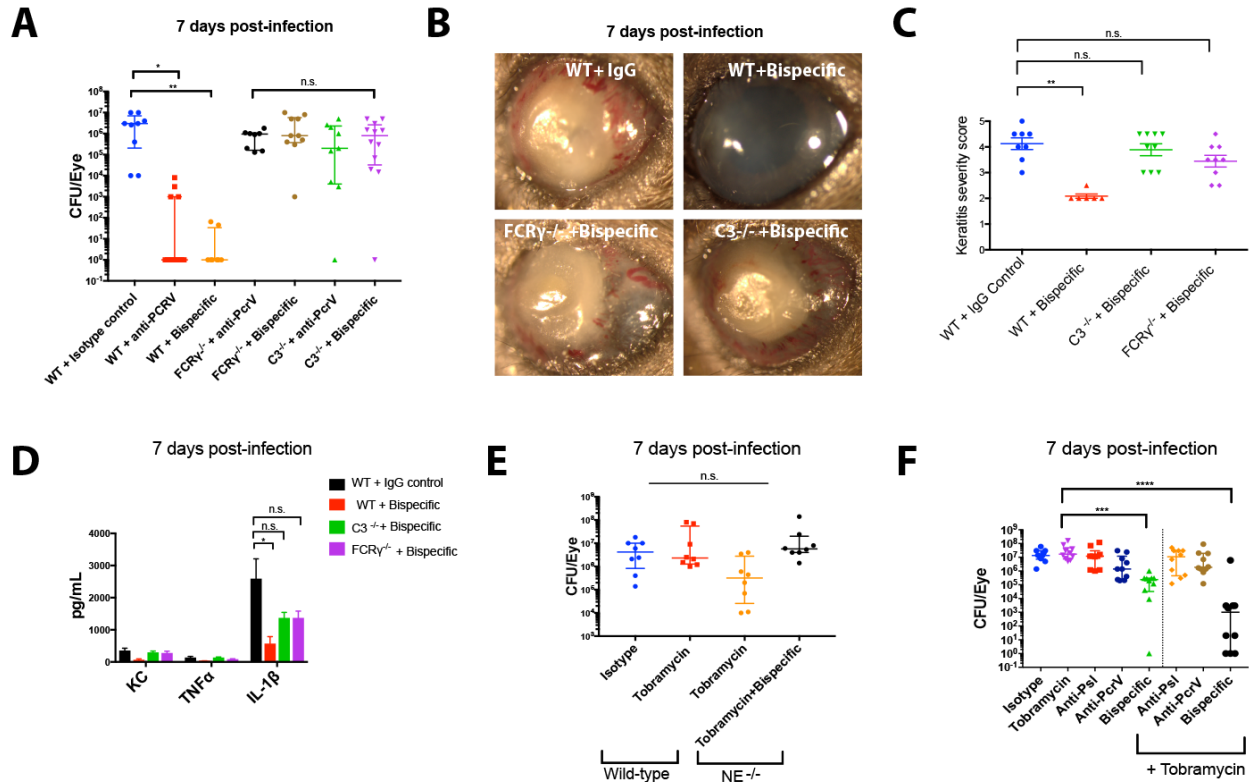


Figure S4. The bispecific antibody requires $C3^{-/-}$ and $Fc\gamma^{-/-}$ to have protective effects in the eye. Related to Figure 4 and 5. **A.** Quantification of bacterial CFUs in eyes of mice infected with PAO1 for 7 days. **B,C.** Eye opacity and keratitis severity score of eyes at day 7 post-infection. **D.** Concentration of pro-inflammatory cytokines and chemokines in eyes at day 7 post-infection. **E.** Quantification of bacterial CFUs in eyes from wild-type C57 and $NE^{-/-}$ mice treated with tobramycin started 6 hours post-infection twice a day for 7 days. **F.** Quantification of bacterial CFUs in eyes after therapeutic treatment with bispecific antibody combined with antibiotics. Data in A, E, and F are represented as median and interquartile range and tested by non-parametric Kruskal-Wallis ANOVA. Data in C and D are represented as the mean \pm standard error and tested by one-way ANOVA. * $p < 0.05$; ** $p < 0.01$, *** $p < 0.001$. $n = 5$ per group.